

See discussions, stats, and author profiles for this publication at: <https://www.researchgate.net/publication/238127227>

# Vapor–Liquid Equilibrium of Binary Mixtures. 2. Ethanol + 2,2,4Trimethylpentane, 1Butanol + 2,2,4Trimethylpentane, and Ethanol + o Xylene

ARTICLE *in* JOURNAL OF CHEMICAL & ENGINEERING DATA · NOVEMBER 2006

Impact Factor: 2.04 · DOI: 10.1021/je060005x

CITATION

1

READS

110

## 5 AUTHORS, INCLUDING:



**Bengt Kronberg**

YKI Institute for Surface Chemistry

86 PUBLICATIONS 2,311 CITATIONS

SEE PROFILE



**Jan van Stam**

Karlstads universitet

68 PUBLICATIONS 1,470 CITATIONS

SEE PROFILE

## Vapor–Liquid Equilibrium of Binary Mixtures. 2. Ethanol + 2,2,4-Trimethylpentane, 1-Butanol + 2,2,4-Trimethylpentane, and Ethanol + *o*-Xylene

Angelica Hull,<sup>\*,†,‡</sup> Bengt Kronberg,<sup>†,‡</sup> Jan van Stam,<sup>‡</sup> Igor Golubkov,<sup>§</sup> and Jan Kristensson<sup>||</sup>

Institute for Surface Chemistry, P.O. Box 5607, SE 114 86 Stockholm, Sweden, Department of Physical Chemistry, Karlstad University, SE 651 88 Karlstad, Sweden, Swedish Biofuels AB, Strandvägen 5B, SE 11451 Stockholm, Sweden, and Chemik Lab AB, P.O. Box 10840 Gribby, SE 76172 Norrtälje, Sweden

The activity coefficients of the binary mixtures ethanol + 2,2,4-trimethylpentane, 1-butanol + 2,2,4-trimethylpentane, and ethanol + *o*-xylene were determined at temperatures of (308.15, 313.15, and 318.15) K. The determination of the vapor phase composition at equilibrium was carried out using headspace gas chromatography analysis. Multiple headspace extraction was used to calibrate the headspace gas chromatograph. Comparison of the experimental phase diagrams with phase diagrams from the literature shows good agreement. The composition of the azeotropes are reported, where they exist. The molar Gibbs energy of mixing is reported for all mixtures studied. The infinite dilution activity coefficients are reported for all components of all mixtures. Some thermodynamic models (those of Wilson, NRTL, UNIQUAC, and Flory–Scatchard) have been compared with regard to their suitability for modeling the experimental data.

### Introduction

The reasons for studying mixtures of hydrocarbons and oxygen-containing compounds relating to the use of oxygen-containing compounds in motor fuels have been presented in our companion paper.<sup>1</sup> Further mixture data are presented here. Part 1<sup>1</sup> includes a description of the experimental techniques and a comparison of the experimental data with literature data. Further comparison with literature data is included in this work. This work extends part 1<sup>1</sup> with a calculation of the molar Gibbs energy of mixing and the infinite dilution activity coefficients for the mixtures studied. An investigation into the suitability of a variety of models for mixtures of hydrocarbons and oxygen-containing compounds is also included.

### Experimental Section

Most of the experimental details have been reported in our companion paper.<sup>1</sup> It is necessary to include here details of the materials used. Also final experimental details on the verification procedures are discussed.

**Materials.** The reagents 1-butanol, 2,2,4-trimethylpentane, and *o*-xylene with a main substance content of not lower than 99.8 % were obtained from Merck. Ethanol 99.7 % volume was obtained from Solveco Chemicals AB. All these reagents were used without additional purification. In addition, chromatographic analysis of the reagents did not reveal any detectable admixtures.

**Verification Tests.** Two verification tests, the integral test and the point test, described in Gmehling and Onken<sup>2</sup> are generally applied to vapor equilibrium data. These tests check for the overall consistency of the data and are well-known. The

more stringent test is the point test, which was applied to the experimental data reported here and in our companion paper.<sup>1</sup>

The point test compares experimental values of the vapor phase composition with those obtained from fitting the data to a Legendre polynomial series of the form of eq 12 in ref 1. As originally described (see also ref 3), the objective function for determining the coefficients of the series is based on pressure data as a function of liquid mole fraction. The same could be done here, but since the pressure results from the combination of the activities of the components of the mixtures, it is more appropriate to construct an objective function based on both sets of activity data as a function of liquid mole fraction. This has the added advantage of using all the experimental information available and avoids the loss of information that would be inherent in using a weight-averaged thermodynamic variable such as pressure or excess Gibbs energy.

A further consideration is the exact form of the activity that should be used. It is customary to use the natural logarithm of the activity coefficient rather than the activity itself for use in equations of chemical potential, Gibbs energy, etc. Accordingly, the objective function  $G$  is constructed on the natural logarithm of the activity coefficients  $\ln \gamma_i$  rather than the activities  $a_i$ :

$$G = \sum_{i=1}^2 \sum_{j=1}^N (\ln \gamma_{ij} - \ln \gamma_i(x_{1j}))^2 \quad (1)$$

where  $\gamma_{ij}$  is the activity coefficient of component  $i$  of data point  $j$ ,  $\ln \gamma_i(x_{1j})$  is the natural logarithm of the value of the activity coefficient functions defined in eqs 13 and 14 of ref 1 evaluated for the liquid mole fraction of component 1 of data point  $j$ , and  $N$  is the number of data points. The objective contains a double summation, so it is applied equally to both activity coefficients of the mixture. The objective function is quadratic in the series coefficients so standard least-squares techniques minimizing  $G$  are used to determine them.

\* Corresponding author e-mail: angelica.hull@surfchem.kth.se.

<sup>†</sup> Institute for Surface Chemistry.

<sup>‡</sup> Karlstad University.

<sup>§</sup> Swedish Biofuels AB.

<sup>||</sup> Chemik Lab AB.

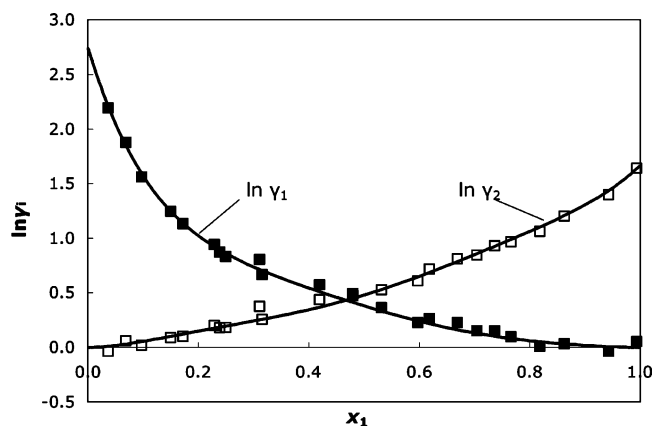


**Figure 1.** Semilog plot of the Legendre series fit to activity coefficient data for the mixture 1-butanol (1) + 2,2,4-trimethylpentane (2) at  $T/K = 313.15$ . The values of the coefficients are in Table 4: ■,  $\gamma_1$ ; □,  $\gamma_2$ .

The result of a typical fit of the data using the first five terms of eq 12 of ref 1 is shown in Figure 1 for the mixture 1-butanol + 2,2,4-trimethylpentane at 313.15 K. The two curves use the same set of coefficients, as they ultimately derive from the same equation, that of eq 12 of ref 1. Five terms were chosen to obtain a sufficiently close fit to the data without overfitting.

Having obtained a fit to the experimental data, the vapor mole fractions are obtained with eq 7 of ref 1 with the pressure obtained from the fitted function rather than the experimental data. The point test as described<sup>2</sup> is then given by the value of the point test consistency parameter  $\epsilon$ :

$$\epsilon = \frac{1}{N} \left| \sum_{i=1}^N y_i - y(x_{1i}) \right| \quad (2)$$

where  $y_i$  is the value of the vapor mole fraction of component 1 of data point  $i$  and  $y(x_{1i})$  is the value of the vapor mole fraction using the fitted function approximation evaluated at the data point  $i$ . The data set is considered to be consistent for a value of  $\epsilon < 0.01$ .

Despite these results, it must be pointed out that no direct measurement of the vapor pressure has been made, for which the point test was originally conceived. Nevertheless the measurements of the activity coefficient of each component in the mixture are independent, so the test provides a measure of the consistency of these data. The relatively small values of  $\epsilon$  reported may derive from the fact that the data are obtained from the same piece of equipment.

**Results.** The additional calibration factors required for 2,2,4-trimethylpentane and *o*-xylene were determined according to the procedure described in ref 1. Figure 2 shows the results of multiple headspace extractions for 2,2,4-trimethylpentane, *o*-xylene, and 1-butanol. The calibration factors obtained using eq 4 of ref 1 are given in Table 1 of ref 1.

Tables 1 to 3 contain the experimental data for the binary mixtures ethanol + 2,2,4-trimethylpentane, 1-butanol + 2,2,4-trimethylpentane, and ethanol + *o*-xylene at temperatures of (308.15, 313.15, and 318.15) K. The liquid mole fraction  $x_1$  of the first component was obtained from the known composition of the sample. The vapor mole fraction  $y_1$  was obtained using eq 6 of ref 1. The activity coefficients of both components,  $\gamma_1$  and  $\gamma_2$ , were obtained using eq 8 of ref 1. The tables include the standard deviation using eq 10 of ref 1 and the value of the point test consistency parameter using eq 2. Tables 1 to 3 contain the experimental data necessary for the calculation of the activity and other physical chemical parameters of the mixtures studied.

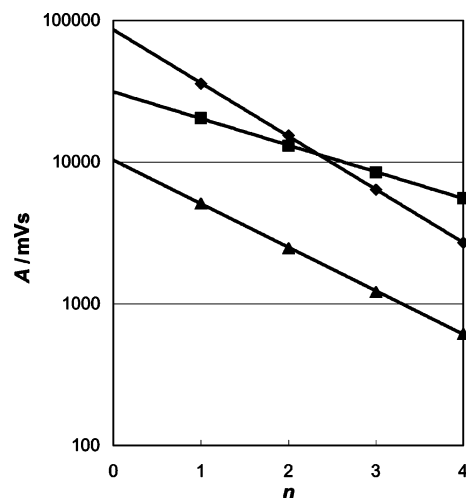


**Figure 2.** Semilog plot of multiple headspace extraction data where the peak area  $A$  is shown in terms of the extraction number  $n$ . The lines are least-squares linear approximations to the data: ■, *o*-xylene; ▲, 1-butanol; ◆, 2,2,4-trimethylpentane.

**Table 1.** Experimental Data for the Binary Mixture Ethanol (1) + 2,2,4-Trimethylpentane (2), Liquid Mole Fraction  $x$ , Vapor Mole Fraction  $y$ , and Activity Coefficient  $\gamma$  at Temperature  $T$ , Standard Deviation  $\sigma$ , and Point Test Consistency  $\epsilon$

$x_1$	$y_1$	$\gamma_1$	$\gamma_2$	$x_1$	$y_1$	$\gamma_1$	$\gamma_2$
$T/K = 308.15$ , $\sigma = 0.037$ , $\epsilon = 0.0035$							
0.056	0.436	9.463	0.959	0.779	0.592	1.141	3.663
0.154	0.500	4.402	1.057	0.817	0.611	1.060	3.964
0.199	0.510	3.504	1.102	0.841	0.630	1.093	4.466
0.240	0.519	3.096	1.193	0.861	0.648	1.071	4.735
0.329	0.527	2.215	1.289	0.893	0.669	1.034	5.655
0.431	0.532	1.729	1.518	0.915	0.701	1.027	6.228
0.546	0.540	1.468	1.982	0.941	0.748	0.974	6.972
0.611	0.548	1.316	2.247	0.950	0.773	1.030	7.577
0.664	0.557	1.316	2.728	0.964	0.811	1.034	8.541
0.744	0.585	1.199	3.264	0.972	0.836	1.027	9.269
0.756	0.588	1.167	3.339	0.976	0.858	1.038	9.169
0.776	0.597	1.116	3.436	0.989	0.922	0.954	9.672
$T/K = 313.15$ , $\sigma = 0.058$ , $\epsilon = 0.0036$							
0.056	0.444	9.021	0.927	0.756	0.590	1.225	3.653
0.105	0.484	6.459	1.120	0.779	0.610	1.168	3.637
0.154	0.504	5.033	1.247	0.817	0.623	1.152	4.302
0.199	0.515	3.796	1.227	0.841	0.640	1.171	4.812
0.240	0.525	3.159	1.242	0.861	0.644	1.177	5.546
0.279	0.530	2.996	1.415	0.893	0.682	1.035	5.593
0.329	0.541	2.397	1.383	0.905	0.697	1.073	6.171
0.431	0.544	1.989	1.743	0.925	0.727	1.122	7.192
0.481	0.548	1.847	1.952	0.941	0.761	1.004	7.007
0.546	0.556	1.470	1.950	0.950	0.779	1.062	7.884
0.603	0.559	1.452	2.399	0.967	0.828	1.053	8.797
0.641	0.567	1.269	2.393	0.976	0.865	1.046	9.082
0.722	0.586	1.190	3.019	0.989	0.930	1.037	9.816
$T/K = 318.15$ , $\sigma = 0.046$ , $\epsilon = 0.0082$							
0.056	0.432	8.892	1.001	0.699	0.582	1.217	2.934
0.105	0.491	6.226	1.101	0.750	0.596	1.179	3.468
0.154	0.514	4.579	1.142	0.779	0.610	1.027	3.350
0.199	0.526	3.761	1.218	0.817	0.639	1.058	3.859
0.240	0.535	3.242	1.281	0.861	0.666	1.080	4.835
0.279	0.541	2.644	1.250	0.893	0.691	1.012	5.483
0.329	0.548	2.333	1.367	0.905	0.714	0.982	5.442
0.431	0.557	1.907	1.658	0.925	0.739	1.007	6.325
0.481	0.562	1.683	1.759	0.946	0.779	1.019	7.289
0.546	0.566	1.317	1.754	0.962	0.821	1.010	8.108
0.611	0.577	1.258	2.092	0.966	0.834	1.022	8.381
0.664	0.582	1.325	2.724	0.989	0.932	1.023	9.832

## Discussion

**Phase Diagrams.** Table 4 lists the coefficients for fitting the data of this work and ref 1 using the procedure described in the Verification Tests section. The complete phase diagrams of the mixtures in this study are shown in Figures 3 to 5. The data

**Table 2.** Experimental Data for the Mixture 1-Butanol (1) + 2,2,4-Trimethylpentane (2), Liquid Mole Fraction  $x$ , Vapor Mole Fraction  $y$ , and Activity Coefficient  $\gamma$  at Temperature  $T$ , Standard Deviation  $\sigma$ , and Point Test Consistency  $\epsilon$ 

$x_1$	$y_1$	$\gamma_1$	$\gamma_2$	$x_1$	$y_1$	$\gamma_1$	$\gamma_2$
$T/K = 308.15, \sigma = 0.036, \epsilon = 0.00086$							
0.037	0.058	9.141	0.974	0.618	0.151	1.249	1.959
0.069	0.071	5.774	0.968	0.669	0.159	1.182	2.165
0.097	0.078	4.592	0.999	0.705	0.167	1.132	2.321
0.150	0.088	3.638	1.141	0.737	0.177	1.148	2.564
0.172	0.089	3.173	1.163	0.801	0.196	1.119	3.175
0.234	0.100	2.521	1.189	0.835	0.218	0.986	3.078
0.313	0.112	2.190	1.361	0.863	0.244	1.013	3.386
0.420	0.129	1.764	1.488	0.891	0.278	0.982	3.612
0.479	0.134	1.596	1.633	0.946	0.406	0.976	4.314
0.510	0.138	1.507	1.688	0.972	0.560	1.021	4.848
0.553	0.142	1.379	1.780	0.994	0.846	1.038	5.312
0.597	0.150	1.365	1.972				
$T/K = 313.15, \sigma = 0.040, \epsilon = 0.0016$							
0.037	0.064	8.964	0.962	0.531	0.156	1.436	1.692
0.069	0.081	6.537	1.062	0.597	0.163	1.254	1.836
0.097	0.088	4.763	1.017	0.618	0.165	1.301	2.048
0.150	0.097	3.472	1.093	0.669	0.178	1.254	2.246
0.172	0.101	3.101	1.106	0.705	0.187	1.165	2.328
0.229	0.107	2.566	1.218	0.737	0.198	1.163	2.532
0.239	0.108	2.388	1.197	0.766	0.209	1.102	2.623
0.249	0.109	2.293	1.200	0.818	0.232	1.008	2.892
0.311	0.118	2.234	1.456	0.863	0.273	1.032	3.325
0.315	0.118	1.948	1.289	0.943	0.429	0.962	4.047
0.420	0.138	1.773	1.545	0.994	0.865	1.053	5.151
0.479	0.148	1.600	1.636				
$T/K = 318.15, \sigma = 0.041, \epsilon = 0.0027$							
0.037	0.071	9.637	1.017	0.618	0.185	1.301	1.985
0.083	0.093	5.406	1.023	0.687	0.200	1.177	2.208
0.161	0.109	3.327	1.113	0.737	0.219	1.125	2.405
0.239	0.119	2.425	1.205	0.783	0.236	1.009	2.527
0.313	0.130	1.997	1.310	0.849	0.284	1.005	3.041
0.420	0.147	1.615	1.448	0.911	0.370	0.983	3.678
0.479	0.167	1.568	1.541	0.943	0.464	0.963	3.917
0.510	0.168	1.591	1.756	0.966	0.578	0.994	4.372
0.553	0.175	1.457	1.816	0.994	0.880	1.001	4.743
0.597	0.181	1.366	1.962				

shown are smoothed data using the Legendre parameters of Table 4 along with eqs 12 to 15 of ref 1 so that the diagrams can be shown as curves rather than individual data points.

The compositions of the azeotropes have been calculated by determining the point of intersection of the bubble and dew curves shown in Figures 3 to 5. The results are shown in Table 5. The alcohol concentration of the azeotropes of the mixtures ethanol + 2,2,4-trimethylpentane and 1-butanol + 2,2,4-trimethylpentane increases slightly with temperature. The mixture ethanol + *o*-xylene does not exhibit an azeotrope for temperatures of (308.15 and 313.15) K but does for 318.15 K. This last result requires further corroboration.

The results of a comparison with the only literature data readily available,<sup>4</sup> the mixture ethanol + 2,2,4-trimethylpentane at a temperature of 313.15 K, are shown in Table 6. The table gives the standard deviation of the distance to the literature data  $\sigma$  in terms of the pressure difference  $[p^e(x_{1i}) - p_i^1]$  between the two sets of data as

$$\sigma = \left( \frac{1}{N} \sum_{i=1}^N [p^e(x_{1i}) - p_i^1]^2 \right)^{1/2} \quad (3)$$

where  $p_i^1$  is the literature vapor pressure value of data point  $i$ ,  $p^e(x_{1i})$  is the value of the experimentally determined vapor pressure fitted function evaluated at the liquid mole fraction of component 1 of the data point  $i$ , and  $N$  is the number of literature data points. Also shown in Table 6 is a comparison of the estimate of the azeotrope for the mixture with good agreement.

**Table 3.** Experimental Data for the Mixture Ethanol (1) + *o*-Xylene (2), Liquid Mole Fraction  $x$ , Vapor Mole Fraction  $y$ , and Activity Coefficient  $\gamma$  at Temperature  $T$ , Standard Deviation  $\sigma$ , and Point Test Consistency  $\epsilon$ 

$x_1$	$y_1$	$\gamma_1$	$\gamma_2$	$x_1$	$y_1$	$\gamma_1$	$\gamma_2$
$T/K = 308.15, \sigma = 0.037, \epsilon = 0.00037$							
0.017	0.539	9.327	0.935	0.485	0.851	1.461	1.610
0.027	0.634	8.670	0.915	0.552	0.864	1.391	1.816
0.052	0.731	7.061	0.962	0.621	0.873	1.194	1.914
0.117	0.792	4.528	1.057	0.678	0.879	1.222	2.370
0.152	0.804	3.613	1.055	0.741	0.890	1.191	2.817
0.183	0.816	3.273	1.107	0.807	0.903	1.060	3.195
0.221	0.822	2.902	1.191	0.874	0.923	1.058	4.110
0.251	0.830	2.503	1.151	0.901	0.932	1.027	4.526
0.254	0.834	2.555	1.160	0.923	0.943	1.017	4.899
0.327	0.841	1.985	1.220	0.962	0.968	1.016	5.725
0.407	0.849	1.752	1.425	0.995	0.995	1.029	6.699
0.435	0.854	1.617	1.428				
$T/K = 313.15, \sigma = 0.057, \epsilon = 0.00046$							
0.016	0.500	8.405	0.934	0.678	0.877	1.196	2.370
0.052	0.727	6.273	0.875	0.743	0.889	1.128	2.729
0.117	0.797	4.933	1.116	0.801	0.900	1.082	3.251
0.183	0.818	3.473	1.167	0.838	0.909	1.064	3.712
0.221	0.832	2.674	1.023	0.865	0.916	1.067	4.203
0.253	0.837	2.328	1.033	0.899	0.931	1.033	4.582
0.327	0.843	2.168	1.322	0.946	0.955	1.016	5.566
0.421	0.853	1.679	1.412	0.964	0.970	0.986	5.632
0.532	0.858	1.387	1.755	0.987	0.987	0.968	6.202
0.639	0.870	1.140	2.024				
$T/K = 318.15, \sigma = 0.058, \epsilon = 0.0060$							
0.010	0.370	8.198	0.981	0.639	0.868	1.275	2.318
0.016	0.472	7.568	0.923	0.678	0.874	1.181	2.408
0.027	0.597	7.938	0.988	0.741	0.882	1.141	2.960
0.117	0.790	4.562	1.082	0.782	0.893	1.046	3.046
0.168	0.810	3.418	1.085	0.801	0.897	1.075	3.363
0.221	0.820	2.713	1.135	0.838	0.906	1.095	3.944
0.253	0.828	2.408	1.136	0.865	0.916	1.118	4.456
0.327	0.837	2.115	1.348	0.883	0.921	1.110	4.801
0.421	0.846	1.689	1.509	0.901	0.932	1.073	4.812
0.485	0.850	1.452	1.628	0.946	0.955	1.090	6.020
0.532	0.857	1.459	1.872	0.964	0.968	1.046	6.236
0.604	0.864	1.248	2.016	0.995	0.995	1.073	7.343

**Table 4.** Legendre Polynomial Series Parameters for the Mixtures of Ref 1 and This Work at Temperature  $T^a$ 

mixture	$T/K$	$a_0$	$a_1$	$a_2$	$A_3$	$a_4$
BI	308.15	1.853	-0.360	0.266	-0.137	0.086
	313.15	1.839	-0.403	0.298	-0.135	0.071
	318.15	1.820	-0.450	0.313	-0.155	0.071
BO	308.15	1.937	-0.321	0.206	-0.068	0.025
	313.15	1.871	-0.392	0.193	-0.060	0.026
	318.15	1.883	-0.359	0.222	-0.067	0.035
EI	308.15	2.284	-0.207	0.343	-0.090	0.069
	313.15	2.335	-0.199	0.266	-0.065	0.030
	318.15	2.266	-0.211	0.311	-0.048	0.062
EO	308.15	2.352	-0.080	0.351	-0.081	0.064
	313.15	2.369	-0.081	0.244	-0.037	0.027
	318.15	2.306	-0.099	0.282	-0.006	0.058
EX	308.15	1.922	-0.188	0.234	-0.057	0.006
	313.15	1.913	-0.144	0.156	-0.046	-0.029
	318.15	1.956	-0.075	0.156	-0.028	-0.020
EB	308.15	-.012				
	313.15	-.056				
	318.15	-.027				

<sup>a</sup> BI, 1-butanol + 2,2,4-trimethylpentane; BO, 1-butanol + octane; EI, ethanol + 2,2,4-trimethylpentane; EO, ethanol + octane; EX, ethanol + *o*-xylene; EB, ethanol + 1-butanol.

**Infinite Dilution Activity Coefficient Values for the Mixtures Studied.** The infinite dilution activity coefficient values for the mixtures studied are readily obtained from the fitted functions  $\gamma(x_1)$  of eq 1 using the Legendre parameters of Table 4 and evaluating them at  $x_1 = 0.1$ . The infinite dilution activity coefficients of the first and second component of the mixture

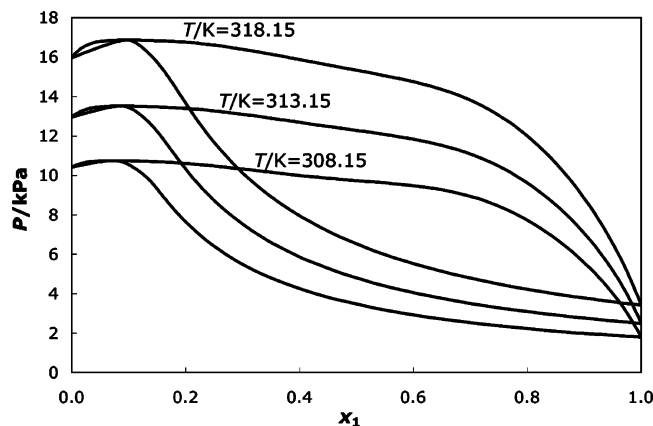


**Figure 3.** Phase diagram of the mixture 1-butanol (1) + 2,2,4-trimethylpentane (2) for the temperatures as indicated. At each temperature there is a pair of curves; the upper one being the bubble point curve and the lower one being the dew point curve. Azeotropes are given in Table 6.

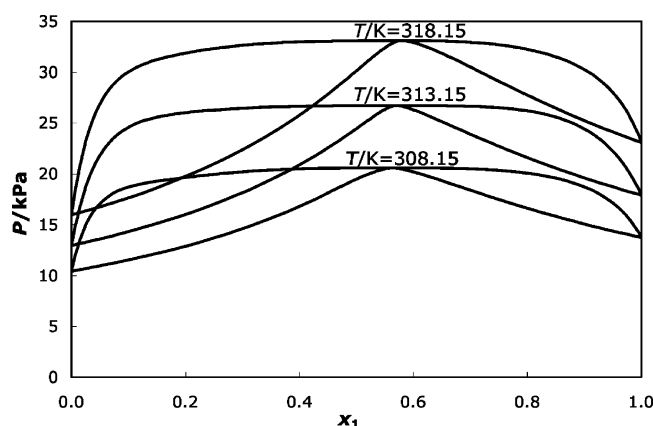


**Figure 4.** Phase diagram of the mixture ethanol (1) + 2,2,4-trimethylpentane (2) for the temperatures as indicated. At each temperature there is a pair of curves; the upper one being the bubble point curve and the lower one being the dew point curve. Azeotropes are given in Table 6.

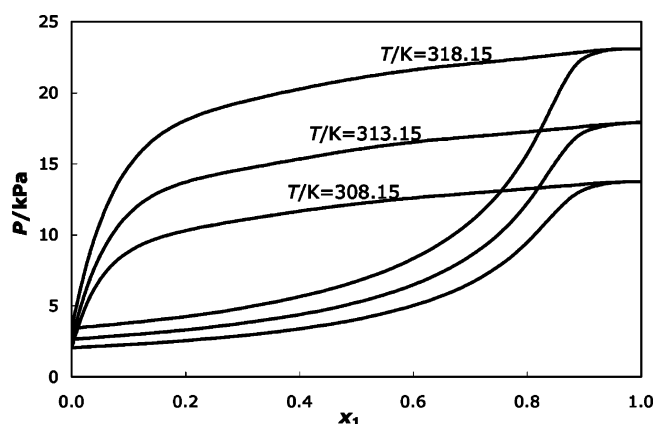


**Figure 5.** Phase diagram of the mixture ethanol (1) + *o*-xylene (2) for the temperatures as indicated. At each temperature there is a pair of curves; the upper one being the bubble point curve and the lower one being the dew point curve. Azeotropes are given in Table 6.

are  $\gamma_1(x_1 = 0)$  and  $\gamma_2(x_2 = 0) = \gamma_2(x_1 = 1)$ , respectively. The values obtained for the mixtures studied are shown in Table 7.

**Gibbs Energy of Mixing for the Mixtures Studied.** The molar Gibbs energy of mixing for all mixtures of this work and ref 1 was calculated based on the experimental data obtained in this study. Figure 6 shows the results for the mixtures ethanol + 1-butanol, ethanol + 2,2,4-trimethylpentane, ethanol + octane, ethanol + *o*-xylene, 1-butanol + 2,2,4-trimethylpentane, and

**Table 5.** Azeotrope Compositions  $x_1$  at Temperature  $T$  of the Mixtures Studied

$T/K$	$x_1$
Ethanol (1) + 2,2,4-Trimethylpentane (2)	
308.15	0.563
313.15	0.570
318.15	0.579
1-Butanol (1) + 2,2,4-Trimethylpentane (2)	
308.15	0.072
313.15	0.086
318.15	0.096
Ethanol (1) + <i>o</i> -Xylene (2)	
308.15	none
313.15	none
318.15	0.981

**Table 6.** Comparison of Experimental Data with Literature Values for the Mixture Ethanol (1) + 2,2,4-Trimethylpentane (2), EI<sup>a</sup>

	$T$	$\sigma$	$x_1$		ref
	K	kPa	(e)	(l)	
EI	313.15	0.144	0.570	0.560	4

<sup>a</sup> Standard deviation  $\sigma$  defined in eq 3. Azeotrope composition  $x_1$  is given for experimental data (e) and literature data (l), which is indicated with the corresponding reference.

**Table 7.** Infinite Dilution Values of the Activity Coefficients for the Mixtures of Ref 1 and This Work<sup>a</sup>

$T/K$	$\gamma_1(x_1 = 0)$	$\gamma_2(x_2 = 0)$
Ethanol (1) + Octane (2)		
308.15	18.7	13.6
313.15	15.8	12.4
318.15	15.6	12.7
1-Butanol (1) + Octane (2)		
308.15	12.9	5.9
313.15	12.7	5.1
318.15	13.0	5.5
Ethanol (1) + 2,2,4-Trimethylpentane (2)		
308.15	19.9	11.0
313.15	18.1	10.7
318.15	18.1	10.8
1-Butanol (1) + 2,2,4-Trimethylpentane (2)		
308.15	14.9	5.5
313.15	15.6	5.3
318.15	16.6	4.9
Ethanol (1) + <i>o</i> -Xylene (2)		
308.15	11.1	6.8
313.15	9.3	6.4
318.15	9.0	7.3
Ethanol (1) + 1-Butanol (2)		
308.15	1.0	1.0
313.15	0.9	0.9
318.15	1.0	1.0

<sup>a</sup> The value for the first component in the mixture corresponds to  $\gamma_1(x_1 = 0)$ , and the value of the second component corresponds to  $\gamma_2(x_2 = 0)$ .

1-butanol + octane at a temperature of 308.15 K. The data shown are smoothed similar to that used for the vapor pressure data of the Phase Diagram section.

Analysis of Gibbs energy for these mixtures shows that the mixture ethanol + 1-butanol has the lowest value of molar Gibbs energy of mixing. The minimum is not shown in Figure 6 but was calculated to be  $-1780 \text{ J} \cdot \text{mol}^{-1}$ . The mixture ethanol + octane has the highest one,  $-368 \text{ J} \cdot \text{mol}^{-1}$ . These results give an indication of the mixing behavior of fuel systems. It is readily apparent from Figure 6 that adding ethanol to octane is considerably more difficult than adding 1-butanol to 2,2,4-trimethylpentane.



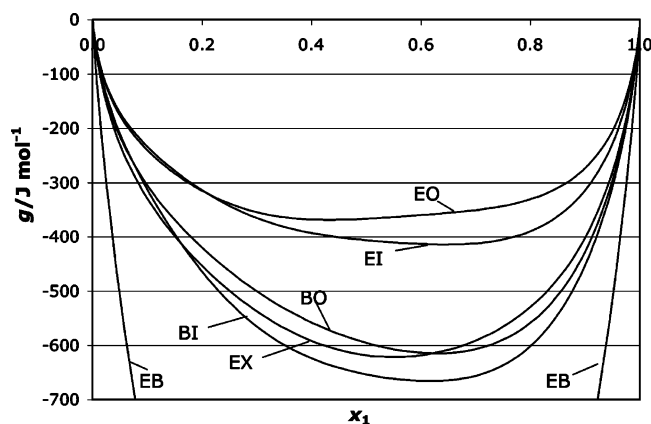


**Figure 6.** Dependence of the molar Gibbs energy of mixing  $g$  on concentration  $x_1$  for binary mixtures at a temperature of 308.15 K: EB, ethanol (1) + 1-butanol (2); BI, 1-butanol (1) + 2,2,4-trimethylpentane (2); BO, 1-butanol (1) + octane (2); EI, ethanol (1) + 2,2,4-trimethylpentane (2); EO, ethanol (1) + octane (2); EX, ethanol (1) + *o*-xylene(2).

### Data Modeling

An investigation of the suitability of various model types for fitting the data was carried out. Simple models such as Porter and Margules do not need to be considered. The types of model are limited to the activity coefficient models of Wilson, NRTL, and UNIQUAC and an association model of the Flory–Scatchard type. The Wilson model is included as it is often used in studies of this kind despite the fact that it does not exhibit a liquid–liquid equilibrium for real-valued parameters.<sup>5</sup>

A baseline from which all the models can be compared has already been established through the earlier procedure of fitting orthogonal series of Legendre polynomials to the data (see the Results section of ref 1). Orthogonal series have the well-known property of successively closer approximation to the data as the number of parameters is increased. There is, however, no physical interpretation of such data fits. The Legendre polynomial fits serve to indicate to what extent the information in the data are fitted by any other model drawn from the list. Each data set was fitted with five terms, and the standard deviation was less than 0.06 in all cases; the actual value of the standard deviation is given in the appropriate experimental table of this work and ref 1. The corresponding Legendre series parameters are given in Table 4. A typical plot of the fit to the data is shown in Figure 1.

The second step was then to attempt to fit each of the models to the data sets. For all the models considered the objective function  $G$  is given by eq 1. The minimization of  $G$  is a nonlinear least-squares problem. The routine to solve this problem uses the Levenburg–Marquardt method to find the best values of the parameters. The quality of fit is calculated as the standard deviation. The results were examined to decide on the best model, that is the one with the smallest standard deviation overall.

**Physical Parameters.** The physical parameters required for the various models are limited to the specification of various molecular parameters, namely, the molar volume, relative surface area, and relative volume taken from Gmehling and Onken.<sup>2</sup>

**Models and Fitting Parameters.** The Wilson model<sup>2</sup> considers the molar volume of each substance and is the simplest model of this kind. The major drawback of the Wilson model is its normally assumed inability to model phase separation.<sup>5</sup> It has two adjustable parameters for each side of a binary interaction. The model parameters, which can be interpreted as

an asymmetric interaction energy, are  $\lambda_{12}$  and  $\lambda_{21}$ :

$$\ln(\gamma_i) = f_i(x; V_i; \lambda_{12}, \lambda_{21}) \quad (4)$$

where  $V_i$  is the molar volume of substance  $i$  and the parameters  $\lambda_{12}$  and  $\lambda_{21}$  are dimensionless interaction energies. The parameters  $\lambda_{12}$  and  $\lambda_{21}$  replace  $(\lambda_{12} - \lambda_{11})/RT$  and  $(\lambda_{21} - \lambda_{22})/RT$ , respectively, in Gmehling and Onken.<sup>2</sup>

The NRTL model<sup>2</sup> corrects the shortcomings of the Wilson model in that it allows the formation of two phases for certain choices of its parameters. It has three adjustable parameters, two of which are dimensionless interaction energies,  $\tau_{12}$  and  $\tau_{21}$ . A third parameter  $\alpha$  accounts for nonrandomness:

$$\ln(\gamma_i) = f_i(x; \tau_{12}, \tau_{21}, \alpha) \quad (5)$$

The UNIQUAC model<sup>2</sup> also corrects the shortcomings of the Wilson model this time by considering the surface area in addition to the volume, for which it uses a relative volume parameter. It has two adjustable parameters, the dimensionless interaction energies  $U_{12}$  and  $U_{21}$ :

$$\ln(\gamma_i) = f_i(x; Q_i, R_i; U_{12}, U_{21}) \quad (6)$$

where  $Q_i$  is the relative molecular area of substance  $i$  and  $R_i$  is the relative volume of substance  $i$ . The parameters  $U_{12}$  and  $U_{21}$  replace  $(u_{12} - u_{22})/RT$  and  $(u_{21} - u_{11})/RT$ , respectively, in Gmehling and Onken.<sup>2</sup>

The Flory–Scatchard model developed by Renon and Prausnitz<sup>6</sup> is the prototypical association model. The alcohol, the associating species, is taken as the first component, and the hydrocarbon as the second component in contrast to Renon and Prausnitz, who have this order reversed. The model parameters are  $K$  (an equilibrium constant) and  $\beta$  (an interaction energy appropriate to a Scatchard model):

$$\begin{aligned} \ln(\gamma_1) = & \frac{(1-x)^2\beta V_1 V_2^2}{RT(xV_1 + (1-x)V_2)^2} + \frac{(1-x)(V_2 - V_1)}{xV_1 + (1-x)V_2} + \\ & \ln \left( \frac{(xV_1 + (1-x)V_2) \left( \frac{2KxV_1}{(xV_1 + (1-x)V_2)} - \sqrt{\frac{4KxV_1}{(xV_1 + (1-x)V_2)} + 1 + 1} \right)}{(2K - \sqrt{4K + 1} + 1)x^2V_1} \right) + \\ & \frac{1}{2K} \left( \frac{2KxV_1}{(xV_1 + (1-x)V_2)} - \sqrt{\frac{4KxV_1}{(xV_1 + (1-x)V_2)} + 1 + 1} \right) \\ \ln(\gamma_2) = & \frac{x^2\beta V_2 V_1^2}{RT(xV_1 + (1-x)V_2)^2} + \frac{x(V_1 - V_2)}{xV_1 + (1-x)V_2} + \ln \left( \frac{V_2}{xV_1 + (1-x)V_2} \right) + \\ & \frac{V_2}{2K V_1} \left( \frac{2KxV_1}{(xV_1 + (1-x)V_2)} - \sqrt{\frac{4KxV_1}{(xV_1 + (1-x)V_2)} + 1 + 1} \right) \end{aligned} \quad (7)$$

where  $R$  is the gas constant,  $T$  is the temperature, and  $V_i$  is the molar volume of substance  $i$ .

A summary of the parameters fitted to the model equations above is shown in Table 8 for each of the 15 mixtures considered. Table 8 presents data for the best-fit parameters and the standard deviation.

**Discussion of the Results.** An overall indication of which models are better can be obtained by summing the root mean squared deviations over all 15 data sets. The results of this are shown in Table 9. The Legendre model is included as the benchmark fit from which all the other models can be compared. Two metrics are shown, the total standard deviation and the total standard deviation relative to the Legendre model fit.

The results of this procedure show a number of interesting features. As expected the orthogonal series fit proves to be an

Table 8. Model Parameters Calculated for the Mixtures Studied<sup>a</sup>

mixture	T/K	Wilson	NRTL	UNIQUAC	Flory–Scatchard
BI	308.15	2.530	0.7241	−0.3334	35.16
		0.2020	0.4967	1.130	5.622
			−1.387		
	313.15	{0.0449}	{0.0457}	{0.0695}	{0.0375}
		2.690	1.068	−0.3872	44.89
		0.1020	2.074	1.229	4.360
	318.15		0.5860		
		{0.0496}	{0.0442}	{0.0800}	{0.0426}
		2.793	1.004	−0.3901	54.88
		0.05941	2.161	1.247	3.287
	318.15		0.5848		
		{0.0486}	{0.0446}	{0.0782}	{0.0422}
		2.579	1.063	−0.3139	36.49
BO	308.15	0.3367	1.884	1.133	7.746
			0.5044		
	313.15	{0.0452}	{0.0463}	{0.0637}	{0.0453}
		2.728	0.8825	−0.3496	63.82
		0.1793	1.902	1.168	4.783
	318.15		0.4863		
		{0.0434}	{0.0434}	{0.053}	{0.047}
		2.609	1.007	−0.3482	38.21
		0.2301	1.926	1.173	6.509
	318.15		0.5250		
		{0.0394}	{0.0397}	{0.0599}	{0.0410}
EI	308.15	3.177	1.621	−0.2068	108.6
		0.4519	2.096	1.534	9.166
			0.4857		
	313.15	{0.0383}	{0.0389}	{0.0737}	{0.0368}
		3.414	0.8701	−0.2278	193.8
		0.4724	0.7340	1.645	8.943
	318.15		−0.9820		
		{0.0584}	{0.0578}	{0.0749}	{0.0584}
		3.197	0.8112	−0.2374	124.8
		0.4044	0.6842	1.610	8.561
	318.15		−1.172		
		{0.0461}	{0.0467}	{0.0758}	{0.0464}
EO	308.15	2.990	1.831	−0.1509	61.49
		0.7486	1.930	1.454	14.22
			0.4732		
	313.15	{0.0410}	{0.0412}	{0.0741}	{0.0397}
		3.200	1.690	−0.1691	99.94
		0.6700	1.863	1.538	12.83
	318.15		0.4321		
		{0.0556}	{0.0517}	{0.069}	{0.0554}
		3.047	1.711	−0.1708	78.36
		0.6271	1.928	1.492	12.56
	318.15		0.4679		
		{0.0333}	{0.0346}	{0.0677}	{0.0364}
EX	308.15	2.469	1.294	−0.2671	22.87
		0.3140	1.777	1.453	12.00
			0.5582		
	313.15	{0.0424}	{0.0373}	{0.0689}	{0.0387}
		2.337	1.211	−0.2235	18.17
		0.3792	1.584	1.343	13.81
	318.15		0.5031		
		{0.0583}	{0.0582}	{0.0681}	{0.0621}
		2.246	1.314	−0.1821	13.83
		0.5274	1.507	1.292	17.72
	318.15		0.4875		
		{0.0590}	{0.0585}	{0.0690}	{0.0628}

<sup>a</sup> BI, 1-butanol + 2,2,4-trimethylpentane; BO, 1-butanol + octane; EI, ethanol + 2,2,4-trimethylpentane; EO, ethanol + octane; EX, ethanol + *o*-xylene. Model parameter order for Wilson,  $\lambda_{12}$ ,  $\lambda_{21}$ ; for NRTL,  $\tau_{12}$ ,  $\tau_{21}$ ,  $\alpha$ ; for UNIQUAC,  $U_{12}$ ,  $U_{21}$ ; for Flory–Scatchard,  $K$ ,  $\beta$ . Values in braces { } are the standard deviations of the fit.

effective benchmark from which the other models can be assessed in the sense that it consistently provides the best fit to the data. It is readily apparent that the Wilson, NRTL, and Flory–Scatchard models perform significantly better than UNIQUAC model for the mixtures considered here. In fact, it was found that the UNIQUAC model is not a significant advance over Margules for low molecular weight alcohol + alkane mixtures. There is nothing to choose from between the Wilson, NRTL, and Flory–Scatchard models as the total relative

Table 9. Summary of Model Comparisons<sup>a</sup>

model	total SD	total relative SD
Legendre	0.6641	15.00
Wilson	0.7034	16.00
NRTL	0.6889	15.66
UNIQUAC	1.045	24.43
Flory–Scatchard	0.6924	15.64

<sup>a</sup> SD, standard deviation.

standard deviation in Table 9 ranges only over 15.64 to 16.0. The benchmark total is 15.0, so these three models are essentially optimal. There would not be any significant observable improvement if a more complicated model were used.

There are two models which incorporate various physical aspects of the molecules of each species, Wilson and UNIQUAC. The Wilson model uses the molar volume, and the UNIQUAC model uses both the surface area and volume ratio relative to water of each molecular species. Although both models are an improvement on regular solution theory, the contrast in the quality of the fit between the Wilson and UNIQUAC models is striking. Generally the Wilson model fits the data as well as the best, but the UNIQUAC model only shows a mediocre performance as compared with Wilson and NRTL. This result has been noted previously by many workers in the field for mixtures of hydrocarbon and alcohol.<sup>2,5</sup> Nevertheless, because the Wilson model does not exhibit phase separation,<sup>5</sup> it cannot be useful for our purposes.

The Flory–Scatchard model, which incorporates the notion of association between the alcohol species and also takes into account the molar volume of each species, shows excellent behavior over all the data sets. This result is somewhat surprising given that the model is not expected to be valid at low concentrations of alcohol.<sup>6</sup> The Flory–Scatchard model has the presumably unphysical characteristic of an infinite activity coefficient for the alcohol in the limit of infinite dilution of the alcohol for the data sets here, but this does not affect the quality of the fit over any nonzero alcohol concentration data. The Flory–Scatchard model as it stands in eq 7 is not suitable for more complicated mixtures than binary. Some work has been reported to extend the model for mixtures of two alcohols and an alkane.<sup>7</sup> A further extension reported in the paper of Campbell<sup>8</sup> is appropriate for any number of alcohols and alkanes.

## Conclusions

The activity coefficients of the binary mixtures ethanol + 2,2,4-trimethylpentane, 1-butanol + 2,2,4-trimethylpentane, and ethanol + *o*-xylene at temperatures of (308.15, 313.15, and 318.15) K have been studied using the method of headspace gas chromatography analysis. Vapor pressures for the binary mixtures ethanol + 2,2,4-trimethylpentane, 1-butanol + 2,2,4-trimethylpentane, and ethanol + *o*-xylene at temperatures of (308.15, 313.15, and 318.15) K have been calculated using the activity coefficients obtained experimentally.

Diagrams of the vapor–liquid phase equilibrium for the binary mixtures ethanol + 2,2,4-trimethylpentane, 1-butanol + 2,2,4-trimethylpentane, and ethanol + *o*-xylene at temperatures of (308.15, 313.15, and 318.15) K have been plotted using the Legendre polynomials for averaging. The molar Gibbs energy of mixing has been calculated for the binary mixtures ethanol + 2,2,4-trimethylpentane, 1-butanol + 2,2,4-trimethylpentane, and ethanol + *o*-xylene at temperatures of (308.15, 313.15, and 318.15) K. It has been established that the mixture 1-butanol + ethanol has the lowest value of Gibbs energy among the

binary mixtures studied and that the mixture ethanol + octane has the highest.

Parameters for the Wilson, NRTL, UNIQUAC, and Flory–Scatchard models have been established for the binary mixtures ethanol + 1-butanol, ethanol + 2,2,4-trimethylpentane, ethanol + octane, ethanol + *o*-xylene, 1-butanol + 2,2,4-trimethylpentane, and 1-butanol + octane at temperatures of (308.15, 313.15, and 318.15) K. The reported lower quality of fit<sup>2,5</sup> of UNIQUAC models for hydrocarbon + alcohol mixtures as compared with other models such as NRTL is confirmed. The Wilson model is unfortunately not suitable for fuel mixtures as it is important for phase separation to be possible. The NRTL and Flory–Scatchard models are clear favorites for modeling hydrocarbon + alcohol mixtures for fuel design purposes. The quality of fit of these models is such that the use of more sophisticated models is not warranted.

### Literature Cited

- (1) Hull, A.; Kronberg, B.; van Stam, J.; Golubkov, I.; Kristensson, J. Vapor–liquid equilibrium of binary mixtures. 1. Ethanol + 1-butanol, ethanol + octane, and 1-butanol + octane. *J. Chem. Eng. Data* **2006**, *51*, 1996–2001.
- (2) Gmehling, J.; Onken, U. *Vapour–Liquid Equilibrium Data Collection I*; Dechema: Frankfurt am Main, 1978.
- (3) van Ness, H. C.; Byer, S. M.; Gibbs, R. E. Vapor–liquid equilibrium: part I. An appraisal of data reduction methods. *AIChE J.* **1973**, *19*, 238–244.
- (4) Ratcliff, G. A.; Chao, K. C. *Can. J. Chem. Eng.* **1969**, *47*, 148–153.
- (5) Elliott, J. R.; Lira, C. T. *Introductory Chemical Engineering Thermodynamics*; Prentice Hall PTR: Upper Saddle River, NJ, 1999.
- (6) Renon, H.; Prausnitz, J. M. On the thermodynamics of alcohol–hydrocarbon solutions. *Chem. Eng. Sci.* **1967**, *22*, 299–307. Errata. *Chem. Eng. Sci.* **1967**, *22*, 1891.
- (7) Pradhan, A. G.; Bhethanabotla, V. R.; Campbell, S. W. Vapor–liquid equilibrium data for ethanol–*n*-heptane–1-propanol and ethanol–*n*-heptane–2-propanol and their interpretation by a simple association model. *Fluid Phase Equilib.* **1993**, *84*, 183–206.
- (8) Campbell, S. W. Chemical theory for mixtures containing any number of alcohols. *Fluid Phase Equilib.* **1994**, *102*, 61–84.

Received for review January 1, 2006. Accepted August 30, 2006. This work was supported by the Swedish Competence Center for Surfactants based on Natural Products (SNAP), Agro Oil AB, and Swedish Biofuels AB.

JE060005X